

Chapter 3

Volume Absorption Coefficients: Instruments, Characterization, Field Measurements and Data Analysis Protocols

Scott Pegau¹, J. Ronald V. Zaneveld¹ and James L. Mueller²

College of Oceanographic and Atmospheric Sciences, Oregon State University, Corvallis

²*Center for Hydro-Optics and Remote Sensing, San Diego State University, California*

3.1 INTRODUCTION

Concepts and methods for measuring the absorption coefficient $a(\lambda)$ of seawater are briefly reviewed in Chapter 1 (Sect. 1.4) of this Volume. Chapter 4 of this Volume is devoted to laboratory spectrophotometric methods of measuring absorption of particles and dissolved materials in filtered water samples. The present chapter focuses on commercially available instruments¹ that may be used from ships and moored platforms to practically measure $a(\lambda)$ in support of satellite validation activities. This first version of absorption protocols is particularly focused on instruments that fall under the “reflective tube” design concept briefly introduced in Sect. 1.4. However, the conceptual basis for determining absorption by measuring flux reflected from a diffuse target is also described later in this section. Expanded reviews of protocols using instruments based on other design concepts are deferred for possible consideration in future revisions to this volume.

Reflective Tube Absorption Meter Concepts

In Sect. 1.4 it was observed that to determine the absorption coefficient associated with transmission over an optical pathlength r_T (Fig. 1.4), it would be necessary to measure the sum of transmitted and scattered flux at the detector, $\Phi_K(r_T) = \Phi_T(r_T) + \Phi_B(r_T)$. Neglecting backscattering, it was suggested that perhaps one might redirect all forward scattered flux to the detector using an *ideal reflective tube*, and determine the absorption coefficient as

$$a = \frac{-1}{r_T} \ln \left(\frac{\Phi_T(r_T) + \Phi_B(r_T)}{\Phi_o(0)} \right). \quad (3.1)$$

Of course a perfectly reflecting tube cannot be realized in a real instrument. Nevertheless, because the scattering phase function of suspended particles in natural waters is strongly peaked in the forward direction (Fig. 1.3), it is possible to use this approach to retain more than approximately 85% of scattered photons in the beam reaching the detector of such an instrument. James and Birge (1938) built a laboratory version of such an instrument to measure absorption spectra of lake waters, and Zaneveld *et al.* (1992) introduced an instrument of this type for *in situ* absorption measurements. In essence, such an instrument is simply a poor transmissometer (Chapter 2) that fails to exclude all of the singly scattered photons from its beam transmittance measurement, and therefore, in its ideal realization would measure only losses due by absorption as per equations (1.9) and (1.10).

The transmittance, absorption, scattering and reflection interaction processes that occur in a real reflective tube absorption meter are illustrated schematically in Fig. 3.1. A source emits collimated flux with a cross sectional area slightly less than that of the reflective tube, and flux reaching the other end of the

¹ Certain commercial equipment, instruments, or materials are identified in this chapter to foster understanding. Such identification does not imply recommendation, or endorsement, by the National Aeronautics and Space Administration, nor does it imply that the materials or equipment identified are necessarily the best available for the purpose.

tube is measured by a detector that covers its entire cross-sectional area. Ray paths extending directly from the source to the detector indicate direct transmittance of flux. Ray paths that terminate within the water volume enclosed by the tube indicate absorbed flux. In natural waters a large fraction of scattered photons are only slightly deflected in the near forward direction (Fig. 1.3) and proceed directly to the large-area detector without encountering the tube walls. Ray paths with scattering angles large enough to encounter the water-quartz interface, where refraction and reflection take place; the refracted portion is transmitted to the outer quartz-air interface, where another refraction and reflection interaction occurs. For simplicity in this conceptual discussion, we do not consider multiple reflection and refractive transmittance interactions within the thin quartz layer. Ray paths containing a scattering angle less than the critical angle ψ_c associated with total internal reflection at the outer quartz-air interface, are totally reflected on each encounter with the tube wall and are transmitted to the detector over a slightly elongated path; for a quartz reflective tube, $\psi_c \cong 42^\circ$, and thus the total internal reflectance represents a very large fraction of all flux scattered by particles (Fig. 1.3). Flux transmitted along ray paths with a scattering angle in the range $\psi_c < \psi < \frac{\pi}{2}$ undergoes partial transmittance losses $[1 - \rho_g(\psi)]$ at each encounter with the reflectance tube, with the reflected portion continuing over a zig-zag path until either reaching the detector or disappearing due to attenuation by absorption and transmission losses in multiple encounters with the tube wall. Flux along ray paths containing a scattering angle $\psi \geq \frac{\pi}{2}$, *i.e.* backscattered flux, is lost from the forward transmittance altogether. Backscattering accounts for only a few percent of scattering by marine particulates (Fig. 1.3).

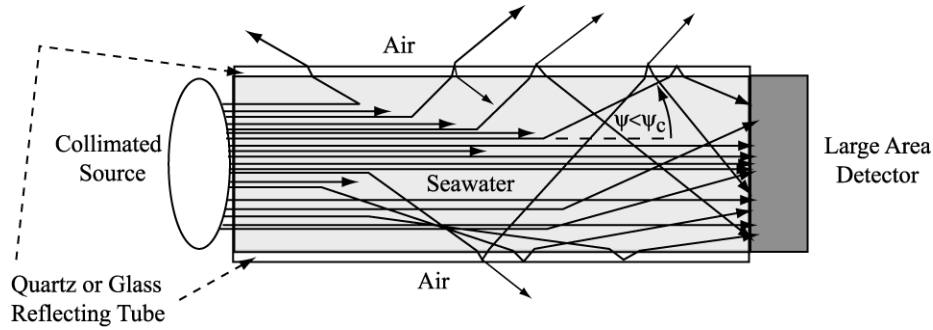


Figure 3.1: Schematic illustration of light interactions and transmission in a reflective tube absorption meter. Ray paths ending in the water represent absorption, and those extending directly from the source to detector represent beam transmittance. Other ray paths indicate scattering interactions: 1) backward scattered paths do not reach the detector, 2) paths with forward scattering at an angle less than the critical angle, *i.e.* $\psi \leq \psi_c$, experience total internal reflection by the tube and reach the detector over an elongated optical path, and 3) forward scattered ray paths at angles in the range $\psi_c < \psi < \frac{\pi}{2}$ experience partial losses from the tube at the quartz-air interface, and may or may not reach the detector depending on whether the internally reflected path survives the absorption process.

In the single scattering approximation, the flux measured by the detector of a reflective tube absorption meter may be written

$$\Phi_m(r_T) = \Phi_T(r_T) + 2\pi\Phi_o(0) \int_0^{r_T} \int_0^{\psi_c} \beta(\psi) e^{-cr} e^{-a \frac{r_T-r}{\cos\psi}} \sin\psi d\psi dr + \quad (3.2)$$

$$2\pi\Phi_o(0) \int_0^{r_T} \int_0^{\psi_c} \beta(\psi) e^{-cr} e^{-a \frac{r_T-r}{\cos\psi}} [\rho_g(\psi)]^{N(r_T-r)} \sin\psi d\psi dr$$

where $\rho_g(\psi)$ is net reflectance of the quartz tube beyond the critical angle, and the exponent $N(r_T - r; \psi)$ is the average number of wall reflections required for a ray path to reach the detector following a scattering event at distance r and angle ψ . The first integral on the right-hand-side of (3.2) represents flux scattered at angles less than the critical over the optical path, and the second integral represents flux reaching the detector following scattering by angles greater than the critical angle. In either case, the pathlength to the detector from a scattering interaction at distance r is $\frac{r_T - r}{\cos \psi}$, and both types of scattered-reflected paths are attenuated by absorption over this elongated path. The second term also is reduced by incomplete reflectance in $N(r_T - r; \psi) \geq 1$ interactions with the reflective tube.

The measured absorption coefficient is therefore greater than the true absorption coefficient since

$$a_m = \frac{-1}{r_T} \ln \left(\frac{\Phi_m(r_T)}{\Phi_o(0)} \right) > a = \frac{-1}{r_T} \ln \left(\frac{\Phi_T(r_T) + \Phi_B(r_T)}{\Phi_o(0)} \right),$$

and the two may be related as

$$a_m = a + 2\pi \int_0^\pi W(\psi) \beta(\psi) \sin \psi d\psi, \quad (3.3)$$

where the weighting coefficients $W(\psi)$ account for the absorption and wall reflection losses in the two integral terms of (3.2) and for the exclusion of backscattering in the measured flux. In other words, the weighting coefficient $W(\psi)$ may be interpreted as the fraction of light that is scattered at angle ψ that does not reach the absorption detector; it may take values from 0, indicating all light scattered at that angle reaches the detector, to 1, indicating that none of the light reaches the detector. The uncertainty of absorption coefficients determined from measurements with a reflective tube instrument is largely determined by the uncertainty of the methods used to correct for the integrated scattering error (Zaneveld *et al.* 1994), which will be briefly summarized below in Sect. 3.4. The remaining sections of this chapter summarize protocols related to characterization, measurement and data analysis using the ac-9 reflective tube absorption meter.

Determination of Absorption by Measuring Flux Reflected from a Diffuse Reflectance Surface

Figure 3.2 illustrates an alternative proposed instrument concept for use in combination with a backscattering meter (Chapter 5) to determine $a(\lambda)$ *in situ*. A divergent source illuminates a diffusely reflecting target oriented parallel to the instrument's window at a fixed distance d_p . An instrument of this type, called the “ α -beta”, is commercially available through HOBILABS, Inc.

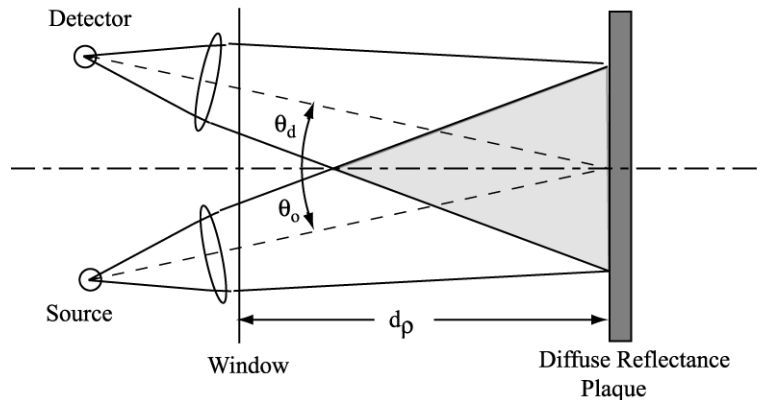


Figure 3.2: Conceptual schematic illustration of an instrument designed to determine the volume absorption coefficient by measuring diffuse reflectance from a plaque. The VSF at

one or more angles must be independently and concurrently measured in this approach. See also Figure 5.1, and the related discussion of calibrating a VSF meter using a diffuse reflecting plaque in Section 5.3, in Chapter 5 of this Volume.

For simplicity in this conceptual discussion, we will assume: 1) that the source beam and detector FOV geometries are identical, 2) that the central viewing angles of each are equal, *i.e.* $\theta_o = \theta_d$ (Fig. 3.2), and 3) that the plaque's Bidirectional Reflectance Distribution Function (BRDF) is a constant $\frac{\rho}{\pi}$. The flux reaching the plaque from the source, including flux scattered in the near forward direction (up to $\sim 15^\circ$ or so) as well as direct transmission, may be expressed as

$$\Phi_r = k_o \Phi_o \exp[-(a + \overset{\frown}{b}_o) \bar{z}], \quad (3.4)$$

where k_o is a constant representing the optical characteristics (reflection and transmission losses, effective detector area, etc.) of the source, \bar{z} is the mean effective pathlength for flux transmitted from the source window to the plaque, $\overset{\frown}{b}_o = b - 2\pi \int_0^{\psi_f} \beta(\psi) \sin \psi d\psi$ is flux scattered beyond a forward scattering angle $\psi_f \leq 15^\circ$ comparable to the beam geometric width. For typical particle phase functions, a very large fraction of singly scattered flux is confined within the forward 15° cone. By similar reasoning, the flux reflected diffusely from the plaque and reaching the detector may be written as

$$\Phi_d = k_d \frac{\rho}{\pi} \Phi_r \exp[-(a + \overset{\frown}{b}_d) \bar{z}] = k_d \frac{\rho}{\pi} k_o \Phi_o \exp[-(2a + \overset{\frown}{b}_o + \overset{\frown}{b}_d) \bar{z}], \quad (3.5)$$

where k_d is a constant accounting for the optical characteristics of the detector assembly, and $\overset{\frown}{b}_d$ represents scattering losses at angles too large to be detected in a single scattering approximation, *i.e.* the counterpart for $\overset{\frown}{b}_o$ for a diffuse source and the detector FOV. Equation (3.5) assumes further that the flux backscattered from the intersection volume of the source beam and detector FOV, the shaded conical region in Fig. 3.2, is negligibly small compared to the flux reflected from the plaque. At this point it may be appropriate for the reader to compare the similarities between the instrument concept illustrated Fig. 2.2 (Chapter 2) and the calibration geometry for determining the weighting function of a VSF, as illustrated in Fig. 5.1, and as described for a plaque reflectance measurement geometry at a fixed distance z as part of the VSF calibration described in Sect. 5.2 (Chapter 5 of this volume) and in Maffione and Dana (1997).

Following the approach used to determine the backscattering coefficient from a measurement $\beta(\psi^*)$ of the VSF at a single angle ψ^* in the backward direction (Chapter 5, Sect. 5.4), Dana, Maffione and Coenen (HOBILabs, Inc., personal comm., *circa* 2000) originally assumed that

$$\overset{\frown}{b}_o + \overset{\frown}{b}_d \cong \chi \beta(\psi^*), \quad (3.6)$$

where χ is an unknown constant. The “ α -beta” instrument designed and manufactured by HOBILabs combines a VSF meter (Chapter 5) to measure $\beta(140^\circ)$ with a device conceptually similar to that illustrated in Fig. 3.2, mounted at opposite ends of a small cylinder.

If the source is regulated to emit constant flux, the system constants of the diffuse reflectance device may be collected as

$$k = F_d k_d \frac{\rho}{\pi} k_o \Phi_o, \quad (3.7)$$

where F_d is the detector assembly's signal responsivity to flux received at the instrument window in water, *i.e.* $F_d = \frac{V_d - V_d^{\text{dark}}}{\Phi_d}$. V_d and V_d^{dark} are the detector flux response and dark response signals, respectively.

Substituting (3.6) and (3.7) allows (3.5) to be rewritten in terms of the dark-corrected detector response $V_d - V_d^{\text{dark}}$ as

$$V_d - V_d^{\text{dark}} = F_d \Phi_d = k \exp\left\{-\left[2a + \chi\beta(\psi^*)\right]\bar{z}\right\},$$

and taking the natural logarithm of both sides and rearranging yields

$$a = \frac{1}{2\bar{z}}\left[\ln(k) - \ln(V_d - V_d^{\text{dark}})\right] - \chi\beta(\psi^*). \quad (3.8)$$

Equation (3.7) contains one unknown variable, a , two measured variables ($V_d - V_d^{\text{dark}}$) and $\beta(\psi^*)$, and three unknown coefficients \bar{z} (the mean effective pathlength between the source, or detector, and reflectance target), k (an overall system optical characteristics constant), and χ (the scaling factor relating the VSF at one angle to the combined sum of backscattering plus forward scattering beyond ψ_f for the two optical paths).

The constant coefficients in (3.8) may be determined by placing the “ α -beta”, or a similar instrument in pure water, and sequentially adding scattering and absorbing materials to increase a , b and $\beta(\psi)$ in $n = 1, 2, K, N$ increments spanning a suitable range of each variable. At each n^{th} incremental step, the reflectance detector response V_{d_n} and VSF measurement $\beta_n(\psi^*)$ are recorded, together with the absorption coefficient $a_n(\lambda)$ measured using a WET Labs ac-9. It is convenient to define two new constants $\gamma = \frac{\ln(k)}{2\bar{z}}$ and $\vartheta = \frac{1}{2\bar{z}}$, and express (3.8) in matrix form for the N sets of measurements as

$$\mathbf{\check{a}} = \mathbf{X}\mathbf{\check{\gamma}}, \quad (3.9)$$

where

$$\mathbf{\check{a}} = \begin{bmatrix} a_1 \\ a_2 \\ \vdots \\ a_N \end{bmatrix}, \quad \mathbf{X} = \begin{bmatrix} 1 & \ln(V_{d1} - V_d^{\text{dark}}) & \beta_1(\psi^*) \\ 1 & \ln(V_{d2} - V_d^{\text{dark}}) & \beta_2(\psi^*) \\ \vdots & \vdots & \vdots \\ 1 & \ln(V_{dN} - V_d^{\text{dark}}) & \beta_N(\psi^*) \end{bmatrix}, \quad \text{and } \mathbf{\check{\gamma}} = \begin{bmatrix} \gamma \\ \vartheta \\ \chi \end{bmatrix}.$$

Multiplying both sides of (3.9) by \mathbf{X}^T , the transpose of the matrix \mathbf{X} , we obtain

$$\mathbf{X}^T\mathbf{\check{a}} = [\mathbf{X}^T\mathbf{X}]\mathbf{\check{\gamma}},$$

leading to the normalized least squares solution for the three coefficients as

$$\mathbf{\check{\gamma}} = [\mathbf{X}^T\mathbf{X}]^{-1} \mathbf{X}^T\mathbf{\check{a}}, \quad (3.10)$$

where $[\mathbf{X}^T\mathbf{X}]^{-1}$ is the inverse of the 3×3 matrix $[\mathbf{X}^T\mathbf{X}]$.

Having thus described the conceptual basis for determining the absorption coefficient from measurements with a HOBILabs “ α -beta” instrument, or a similar instrument, time constraints on the publication schedule for this document preclude exploring more detailed protocols for its calibration and use, or the uncertainty budgets associated with this approach. These considerations must be deferred to a possible future revision to this protocol volume.

3.2 CHARACTERIZATION and CALIBRATION OF REFLECTIVE TUBE SPECTRAL ABSORPTION METERS

Perhaps the best-known version of a reflective tube absorption meter is the ac-9 manufactured by WET Labs, Inc. This instrument measures both the spectral beam attenuation coefficient $c(\lambda)$ in an enclosed

flow-through non-reflective optical path, and the spectral volume absorption coefficient $a(\lambda)$ using parallel enclosed flow-through reflective tube optical paths, one of which (the absorption side) is a reflective tube (Fig. 3.1). Many aspects of the characterization, calibration, field measurements and data analysis protocols relating to this type of instrument were introduced in Chapter 2 and will not be repeated here. Moreover the manufacturer provides extremely detailed protocols for calibrating and using this instrument, and for analyzing its data, both in the ac-9 User Manual, and in a detailed protocol manual (Van Zee *et al.* 2002), both of which are available online (www.wetlabs.com). Additional background information related to characterization, calibration and data analysis methods for this instrument may be found in Moore *et al.* (1992), Zaneveld *et al.* (1992) and Twardowski *et al.* (1999). Here we will briefly highlight critical aspects of the protocols that must be carefully followed to obtain accurate $a(\lambda)$ measurements using this, or a similar, instrument in the field. Many of these topics, as they relate to the beam transmissometer side of the instrument, have been discussed in Chapter 2 of this volume.

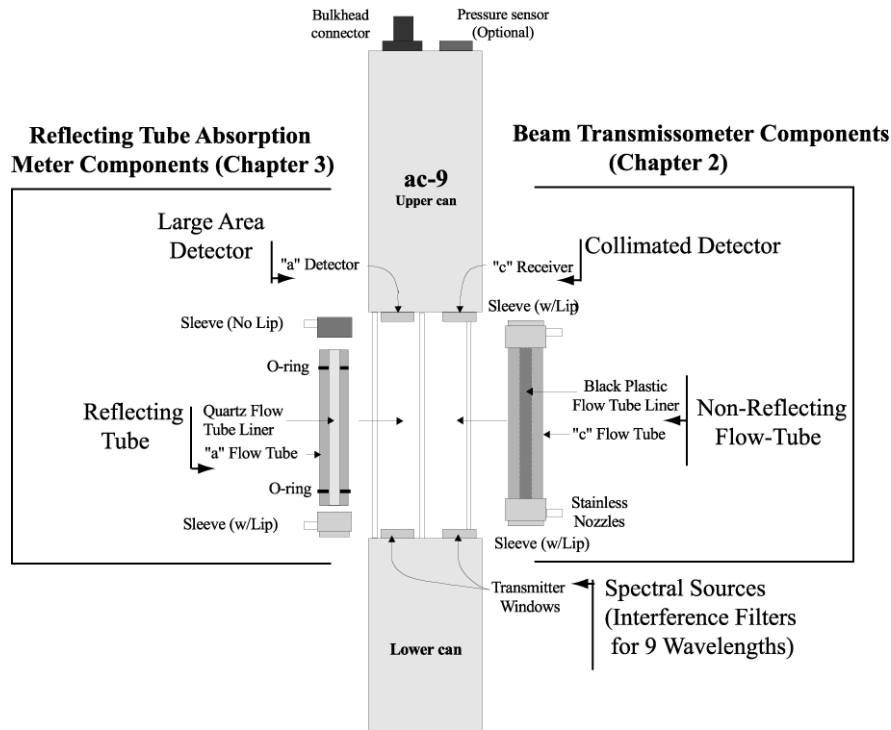


Fig. 3.3 Schematic illustration of the ac-9 beam attenuation and absorption meter (courtesy of WET Labs, Inc).

Pure Water Calibration

The procedure for using pure water to calibrate the reflective tube absorption meter side of an ac-9 is identical to that described in Chapter 2 (Sect. 2.4) for its flow-through beam-transmissometer side. The calibration equation for measured absorption a_m relative to pure water, corresponding to equation (2.9) for c , is

$$a_m(\lambda) - a_w(\lambda) = \frac{1}{r_T} \ln \left\{ \frac{[V_{R,w}(\lambda) - V_{R,w}^{\text{dark}}(\lambda)] [V_D(\lambda) - V_D^{\text{dark}}(\lambda)]}{[V_{D,w}(\lambda) - V_{D,w}^{\text{dark}}(\lambda)] [V_R(\lambda) - V_R^{\text{dark}}(\lambda)]} \right\}, \quad (3.11)$$

where the signal notations on the right-hand-side are the same as those defined in Chapter 2, and pure water absorption values are listed in Table 1.1 of Chapter 1.

Pure Water Preparation

The methods for preparation of optical calibration grade pure water were not addressed in Chapter 2, and are included here.

To prepare pure water for instrument calibrations, the manufacture uses a commercial de-ionization system and filtration system. After primary de-ionization, the water is processed using a Barnstead, or equivalent, purification unit and stored in a large holding tank. To maintain purity, water in the holding tank should be re-circulated through a ultra-violet chamber and additional purification filters. Water for calibration is drawn through a 0.01-micron ultra-filter at the point of delivery. The circulating holding tank allows the highly reactive de-ionized water to equilibrate with the ambient conditions and the ultra-violet chamber prevents any biological contamination from entering the reservoir.

For field calibrations, one approach is to either purchase HPLC grade pure water, or produce it in the lab, and transport it to the ship, especially for short cruises. On some research vessels, a water deionization and purification system is permanently installed to support the scientific party. If so, care must be taken to insure that the filters are fresh and do not produce Colored Dissolved Organic Matter (CDOM) from decaying particles trapped in the filter. Alternatively, a portable system consisting of a commercial filtration unit, such as the Barnstead E-Pure or the Milli-Q Q-Pak treatment systems may be set up temporarily on the ship. The input water should be pre-filtered using a 1.5 μm commercial filter cartridge and an activated charcoal filter to increase the lifetime of the primary unit. Pure water should be produced in advance of the calibration and stored in a clean 20-liter polycarbonate carboy and be allowed to stand for approximately 12 hours to equilibrate with the ambient temperature and to remove bubbles.

To calibrate an ac-9, the carboy may be equipped with a cap having barb fittings to connect tubing to a pressurization unit that pushes water to the instrument (Fig. 3.4). The carboy is pressurized to approximately 10 psi using an oil free air pump, or a tank of dry nitrogen gas. The air supply tube inside the carboy should be kept above the water level to prevent the creation of bubbles when pressurizing the carboy, and the outlet tube should extend nearly to the bottom of the carboy. To connect the carboy to the ac-9, Teflon tubing is recommended, rather than Tygon tubing, which may contain plasticizers that can contaminate the water. The tubing from the carboy is connected to the bottom nozzle on the ac-9 flow tube. The tubing near the ac-9 inlet and outlet should be covered with black tape to avoid ambient light leaks into the optical path. A short piece of tubing with a valve is connected to the top nozzle on the flow tube, both to control water flow through the system, and to provide backpressure, which helps to keep gases in solution and prevents the formation of micro-bubbles. An optional 0.2-micron filter may be placed at the point of delivery.

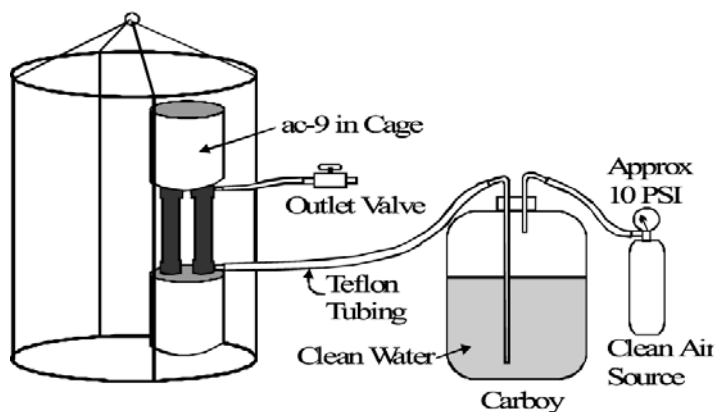


Fig. 3.4. Schematic illustration of a pure-water supply system for field calibrations of an ac-9.

This procedure is discussed adequately in Chapter 2.

3.3 MEASURING SPECTRAL ABSORPTION COEFFICIENTS WITH REFLECTIVE TUBE METERS

The ac-9 should be mounted in a profiling instrument cage following directions provided by the manufacturer (Van Zee *et al.* 2002). It is strongly recommended to mount a CTD data the same profiling package as an ac-9, and to develop a method for accurately merging the measurements from both instruments; combining the data streams from the two instruments in real time as part of the data acquisition system is the preferred approach, with a second choice being to time-tag both data records and merge the data on that basis. The basis of these recommendations is that water temperature and salinity data are essential for the corrections described below in Sect. 3.4.

To begin a cast, place the instrument package in the water before they are powered up. Then hold the package underwater near the surface allow approximately 5 min for the instruments to warm up, stabilize the electronics, and reduce the possibility that thermal shock may adversely affect the measurements. Monitor the instrument outputs and wait to begin profiling until the instrument stabilizes at the surface. If an absorption meter will not stabilize its readings after 5-10 minutes under these conditions, it is recommended that it be returned to the manufacturer for characterization of the problem and necessary repairs.

If possible place the instrument 10 to 20 meters below the surface to help purge bubbles. Purging bubbles is more difficult when making filtered measurements (see below). If you are not making filtered measurements the instruments will generally purge at the surface, but purging them below 10 m is still a good idea.

The reader is referred to Van Zee *et al.* (2002) for detailed recommendations concerning rates of descent during profiles using an ac-9.

After the instruments are brought on deck following a cast, they should be immediately rinsed, and the flow tubes flushed, with fresh water to mitigate corrosion. If the instrument will be on deck for more than 30 min between casts, the optics and flow tubes should be cleaned with Nannopure water and dried. At least once per day, while at sea, the optics and flow tubes should be cleaned with methanol, cleaned again using a mild detergent dissolved in Nannopure water, rinsed with Nannopure water, cleaned again with methanol, and finally dried. Use soft tissues, such as KimWipes, to gently clean and dry the optical surface, and be extremely careful to wipe them in a constant direction and to not scrub the optical surfaces.

When the instrument package is to be stored on deck for a prolonged period between casts, cover it with a tarpaulin to protect the absorption meter from direct exposure to the sun. Excessive solar heating of the instrument may exceed the practical limits (5 °C to 30 °C) of internal temperature corrections for an ac-9, and thus invalidate its measurements until it has cooled sufficiently to restore normal operations.

Filtering the Water Intake Port of an ac-9 for Measurements of Absorption by CDOM and Particles

The absorption coefficient of dissolved material may be measured by attaching a 0.2 µm pore-size filter to the intake of an ac-9. The recommended practice is to locate the intake filter below the instrument at the bottom of the cage. Measurements in the filtered intake configuration are also very useful for testing the operational performance of ac-9; quality control procedures using dissolved measurements are discussed in Sect. 3.5.

Examples of suitable filters are the Gelman Suporcap 100 and Gelman Maxi-cap (0.2 µm) filters. These filters have high flow rates at low differential pressure and don't adsorb or leach materials. The outer housings of these commercial filter cartridges may be cut off to allow some flushing of the filter and increase the flow-rate. Make sure you don't handle the filter material, or lay a filter on the deck, where it can be exposed to oil and grease. Hose clamp the filter to the tubing and make sure any vents on the filter are closed. Before use, a filter should be either flushed for several minutes with DI water, or soaked several hours in DI water, to remove air pockets in the filter membrane. As a note of caution, never flush a filter in the reverse direction!

There are alternative ways to plumb the filters into the ac-9 instrument. The preferred arrangement is to filter the a and c sides separately using two filters and two pumps, so that each side is plumbed independently. This approach is expensive, however, and is not necessary for measuring the absorption by the dissolved component. For measurement of the absorption by dissolved materials, only one side needs to be filtered, because scattering by particles less than $0.2\ \mu\text{m}$ in size is not detectable by an ac-9, and hence the filtered a and c measurements are equal. On the other hand, measurements with filters on intakes of both sides are useful for quality control tests (Sect. 3.5).

If possible replace the filter daily. If you choose to replace a filter less frequently, soak it in DI water during long breaks between profile measurements during a deployment. Record the date of each filter change in the cruise log.

Mixing of water within the filter cartridge will smear measurements of a vertical gradient in the absorption by dissolved materials, and an unfiltered instrument will detect a gradient in total absorption with better vertical resolution. In addition, the reduced flow rate through the filter will increase the time lag to approximately 4 to 6 sec, compared to 1.2 to 1.8 sec for unfiltered measurements. Moreover, the lag rate will gradually increase as a filter accumulates particles during its use. The preferred means of determining flow rate and lag corrections is to attach a flow-meter in-line into the supply or exhaust tubing. An indirect technique for estimating flow-rate related lag times is to match depths of changes in the $a(715)$ channel with depths of strong changes in water temperature; these changes are linked because absorption by water is temperature dependent in the near infrared (Sect. 3.4), and the time lag between matched changes can be derived from the depth separation and the profiler's rate of descent.

A combination of unfiltered and filtered ac-9 measurements can be used to derive particle absorption and attenuation coefficients, as well as absorption by CDOM. There are several combinations that can be used:

- From measurements using a single ac-9 with the c side filtered and the a side unfiltered, particle absorption can be obtained as $a_p(\lambda) = a(\lambda) - a_w(\lambda) - [c_g(\lambda) - c_w(\lambda)]$, where the measurements have been corrected using the methods described in 3.6 below. The subscript “g” is associated with CDOM, based on historical use of the term “gelbstoffe”, or yellow-matter, as a pseudonym of CDOM.
- From measurements with two ac-9's, one filtered and one unfiltered, $a_g(\lambda)$ is derived directly from the filtered measurements, after the corrections of Sect. 3.6, and $a_p(\lambda) = a(\lambda) - a_g(\lambda)$, where $a(\lambda)$ is derived from the unfiltered instrument and the pure water terms cancel. This approach may also be used with a single instrument by making successive casts, one with the filter attached and the second with the filter removed.
- Another alternative approach is to make successive casts with one instrument, filtering the a intake on one cast, and the c intake on the other. The filtered and unfiltered measurements from the two casts are combined as above.

The approach yielding the lowest instrumental uncertainty of the particulate absorption is to derive it from filtered and unfiltered measurements with the same instrument on successive casts. Calibration offsets, whether known or not, are identical in the filtered and unfiltered measurements on each side, and therefore, the offsets cancel when particle absorption is determined as the difference between the two measurements. On the other hand, potentially larger uncertainty may result from possible changes in the IOP profiles between casts, due to horizontal advection and/or vertical displacement of IOP features by internal waves.

3.6 DATA ANALYSIS METHODS

The initial steps in processing absorption measurements using an ac-9 reflective tube absorption meter are identical to those presented for processing beam transmissometer measurements in Chapter 2, Sect. 2.5 [substituting equation (3.11) for (2.9) in Step 4]. This information will not be repeated here. Two additional analysis steps are necessary to obtain accurate absorption coefficients from combined ac-9, or

similar instrument, measurements of $a_m(\lambda)$ and $c_m(\lambda)$: 1) corrections for water temperature and salinity induced offsets in water absorption and attenuation, and 2) corrections for scattering errors [equation (3.3)] in $a_m(\lambda)$.

Temperature and Salinity Corrections

The absorption of pure water is dependent on water temperature T [$^{\circ}\text{C}$] (Pegau and Zaneveld 1993) and the absorption coefficient of seawater is also dependent on its salinity S [PSU] (Pegau *et al.* 1997). These variations affect the measured coefficients of absorption $a_m(\lambda)$ and attenuation $c_m(\lambda)$ in the following ways:

1. The difference $(T - T_r)$ between the water temperature T during a measurement at sea and the temperature T_r of the pure water reference standard at the time the instrument was calibrated changes the water absorption “baseline” value $a_w(\lambda)$. This change affects $a_m(\lambda)$ and $c_m(\lambda)$ equally, because scattering by pure water is not significantly temperature dependent.
2. The absorption of seawater varies with salinity S , and of course $S = 0$ PSU for the pure water reference standard used to calibrate the ac-9. This additional shift in the water-absorption “baseline” also affects $a_m(\lambda)$ and $c_m(\lambda)$ equally.
3. The salinity dependent variations in the refractive index of seawater affect the transmission of the optical windows, and the effects are different for the windows of the absorption and beam transmission sides of the instrument. This effect may also vary slightly between instruments (Van Zee *et al.* 2002).
4. Therefore, separate coefficients $\frac{\partial a(\lambda)}{\partial S}$ and $\frac{\partial c(\lambda)}{\partial S}$ combine salinity dependent instrument characteristics and water-absorption variations (Pegau *et al.* 1997; Van Zee *et al.* 2002), and must be applied separately to correct to $a_m(\lambda)$ and $c_m(\lambda)$

The temperature and salinity corrections are applied to measured absorption as

$$a_m^{TS}(\lambda) = a_m(\lambda) - \frac{\partial a_w(\lambda)}{\partial T}(T - T_r) - \frac{\partial a(\lambda)}{\partial S}S, \quad (3.12)$$

and to measured beam attenuation as

$$c_m^{TS}(\lambda) = c_m(\lambda) - \frac{\partial a_w(\lambda)}{\partial T}(T - T_r) - \frac{\partial c(\lambda)}{\partial S}S. \quad (3.13)$$

The temperature dependence coefficients are listed in Table 1.1 (Pegau and Zaneveld 1993; Pegau *et al.* 1997), and the salinity dependence coefficients are provided by the manufacturer (Van Zee *et al.* 2002). Temperature and salinity must be measured, using a CTD, concurrently with an ac-9 profile to apply these corrections using (3.12) and (3.13). Therefore, it is strongly recommended that the ac-9 be mounted on the same profiling package as an accurate CTD, and from this perspective, the priority of CTD measurements is higher than is implied in Table 3.1 (Vol. I, Chapter 2).

These corrections become directly significant only at red and near-infrared wavelengths (see Table 1.1). However, the methods of the next section depend on accurate values of $a_m^{TS}(\lambda_{\text{NIR}})$ and $c_m^{TS}(\lambda_{\text{NIR}})$ at a near-infrared reference wavelength $\lambda_{\text{NIR}} \approx 715$ nm to determine *scattering corrections* at all wavelengths. Moreover, the temperature correction in (3.12) must also be applied to laboratory spectrophotometric measurements of absorption by CDOM (Chapter 4), if the temperatures of the pure-water reference blank and filtered seawater sample differ significantly.

Scattering Corrections

The systematic scattering offsets between true absorption and absorption measured with a reflective tube instrument, as described in equations (3.2) and (3.3) and related text in Sect. 3.1, were evaluated by Zaneveld *et al.* (1994). They recommended a hierarchy of three alternative methods for correcting the scattering offsets to the temperature and salinity corrected measured absorption $a_m^{TS}(\lambda)$:

1. Subtract the measured absorption at a near infrared reference wavelength, *e.g.* $\lambda_{\text{NIR}} \approx 715$ nm for an ac-9, or $\lambda_{\text{NIR}} \approx 750$ nm for measurements with a laboratory spectrophotometer (Chapter 4). After first applying the *temperature and salinity* corrections using (3.12) and (3.13), assume that the $a(\lambda_{\text{NIR}}) - a_w(\lambda_{\text{NIR}}) \approx 0$ and that the entire measured signal at the reference wavelength is due to wavelength independent scattering errors, so that

$$a(\lambda) - a_w(\lambda) = a_m^{TS}(\lambda) - a_m^{TS}(\lambda_{\text{NIR}}). \quad (3.14)$$

The value of $a_m^{TS}(\lambda_{\text{NIR}})$ should be reported with the corrected absorption values when this method is used.

2. Assuming a wavelength-independent scattering phase function appropriate for the type of particulates in a given water mass, and a weighting function $W(\psi)$ based on instrument characteristics [see equation (3.3) and the preceding discussion in Sect. 1.1 above], estimate the scattering error as a fraction ε of the measured scattering coefficient, and subtract it from the measured absorption at each wavelength, *i.e.*

$$a(\lambda) - a_w(\lambda) = a_m^{TS}(\lambda) - \varepsilon [c_m^{TS}(\lambda) - a_m^{TS}(\lambda)]. \quad (3.15)$$

Based on analyses of field measurements, laboratory experiments using an ac-9, and theoretical calculations (Kirk 1992), the fraction ε varies from approximately 0.14 for predominately biological particles in the open ocean (Case 1 waters) and increases to approximately 0.18 in waters where scattering is dominated by suspended sediments (Case 2 waters). Note that although the scattering correction using (3.15) is not sensitive to temperature and salinity corrections at wavelengths < 650 nm, it is nevertheless strongly recommended that the temperature and salinity corrected values be used here as well - if for no other reason than facilitating quality control comparisons between corrections made by different methods.

3. Combine methods 1 and 2, and the assumptions underlying both methods, to use the ac-9 measurements at the reference wavelength to determine ε , so that (3.15) becomes

$$a(\lambda) - a_w(\lambda) = a_m^{TS}(\lambda) - \left[\frac{a_m^{TS}(\lambda_{\text{NIR}})}{c_m^{TS}(\lambda_{\text{NIR}}) - a_m^{TS}(\lambda_{\text{NIR}})} \right] [c_m^{TS}(\lambda) - a_m^{TS}(\lambda)]. \quad (3.16)$$

The ac-9 instrument design constrains the scattering error fraction to $\varepsilon \geq 0.07$ (Kirk 1992), and although it is theoretically possible for ε to reach values exceeding 0.5, the authors have not encountered values greater than 0.35.

The choice of which method should be used to correct scattering errors in ac-9 absorption measurements depends largely on the combination of measured variables, the uncertainty of each measurements, and a judgment of how likely the assumption that $a(\lambda_{\text{NIR}}) - a_w(\lambda_{\text{NIR}}) \approx 0$ is true in a given water mass.

1. It is strongly recommended to use Method 3 to apply the scattering correction, if all variables in (3.16) have been measured with acceptable uncertainty, and there is no reason to suspect that particle absorption is significant at the near-infrared reference wavelength λ_{NIR} .
2. Method 2 is recommended if both $a_m^{TS}(\lambda)$ and $c_m^{TS}(\lambda)$ are available at one or more visible wavelengths, but $a_m^{TS}(\lambda_{\text{NIR}})$ and $c_m^{TS}(\lambda_{\text{NIR}})$ either were not measured with acceptable uncertainties, or there is reason to suspect that $a(\lambda_{\text{NIR}}) - a_w(\lambda_{\text{NIR}}) > 0$.

3. Method 1 must be used if only $a_m^{TS}(\lambda)$ and $a_m^{TS}(\lambda_{NIR})$ are measured, as for example, when a laboratory benchtop spectrophotometer is used to measure $a_g(\lambda)$ in filtered water samples (Chapter 4). This situation might also occur if the *c* side data of an ac-9 were lost due to an electronic failure, or blockage of its flow-tube, and one wished to salvage the absorption profile measured with that instrument.

3.7 QUALITY CONTROL PROCEDURES

There are several quality assurance tests that can be made to check how well an ac-9 is operating.

When using intake filters for quality control measurements in tests of instrument performance, it is best to filter both sides of an ac-9. This can be done by filtering one side at a time, and doing multiple profiles, or by connecting a single filter and pump to both sides of the ac-9. When connecting to both sides using a single filter you are reducing an already low flow, which makes it more difficult to remove bubbles from the system, but it requires fewer casts to complete an instrument test. A degassing Y may be used on the outflow side of the combined plumbing arrangement to facilitate bubble removal.

The noise level in the measurements should be $>0.005 \text{ m}^{-1}$ at all channels. Measurements with noise exceeding this criterion indicate instruments with large measurement noise, a rough check of quality of the calibration, and pressure or temperature dependencies that may exist.

Assuming that there is no measurable scattering by particles that pass through the filter then the filtered *a* and *c* measurements should be equal, and departures $>0.005 \text{ m}^{-1}$ are symptoms of drift in pure water calibration offsets, or calibration errors due to optical impurity of the reference water.

Comparisons of profiles between successive down and up casts may help in separating suspected temperature effects from pressure dependencies. Evidence of hysteresis in different up and down profile responses to gradient features is symptomatic of a problem with an instrument's internal temperature compensation. Care must be taken in this interpretation, however, because the upcast water intake is taken in the wake of the rising package and turbulence may also cause apparent hysteresis symptoms to appear in the measurements. Pressure effects should not have hysteresis.

If more than one ac-9 is available, it is useful to plumb both instruments in identical configurations (both with, or without an intake filter) on the same instrument and measure a quick sequence of comparative profiles to intercalibrate the instruments. The profile data from the two instruments should be compared only after each has been fully processed and corrected for temperature, salinity and scattering errors (Sect. 3.4). Discrepancies in this type of comparison cannot indicate which instrument is incorrect, but does provide a clear indication that the calibration of one, or both, is not correct.

REFERENCES

- James, H.R., and E.A. Birge, 1938: A laboratory study of the absorption of light by lake waters. *Trans. Wis. Acad. Sci.*, **31**: 1--154.
- Kirk, J.T.O., 1992. Monte Carlo modeling of the performance of a reflective tube absorption meter. *Appl. Opt.* **31(30)**: 6463-6468.
- Moore, C., J.R.V. Zaneveld and J.C. Kitchen, 1992: Preliminary results from an *in situ* spectral absorption meter, *Ocean Optics XI, Proc. SPIE* **1750**: 330-337.
- Maffione, R.A. and D.R. Dana, 1997: Instruments and methods for measuring the backward-scattering coefficient of ocean waters. *Appl. Opt.* **36**: 6057-6067.
- Pegau, W.S. and J.R.V. Zaneveld, 1993: Temperature dependent absorption of water in the red and near infrared portions of the spectrum. *Limnol. Oceanogr.*, **38(1)**: 188-192.
- Pegau, W.S., D. Gray and J.R.V. Zaneveld, 1997: Absorption and attenuation of visible and near-infrared light in water: dependence on temperature and salinity. *Appl. Opt.*, **36(24)**: 6035-6046.

- Twardowski, M.S., J.M. Sullivan, P.L. Donaghay and J.R.V. Zaneveld. 1999: Microscale quantification of the absorption by dissolved and particulate material in coastal waters with an ac-9. *J. Atmos. Oceanic Tech.* **16**: 691-707.
- Van Zee, H., D. Hankins, and C. deLespinasse, 2002: *ac-9 Protocol Document (Revision F)*. WET Labs Inc., Philomath, OR, 41pp.
- Zaneveld, J.R.V., J.C. Kitchen, A. Bricaud, and C. Moore, 1992: Analysis of *in situ* spectral absorption meter data. *Ocean Optics XI*, G.D. Gilbert, Ed., SPIE, 1750, 187--200.
- Zaneveld, J.R.V., J.C. Kitchen, and C. Moore, 1994: The scattering error correction of reflecting-tube absorption meters. *Ocean Optics XII, Proc. SPIE*, **2258**: 44-55.